Journal of Non-Crystalline Solids 453 (2016) 23–27

Contents lists available at ScienceDirect

Journal of Non-Crystalline Solids

journal homepage: www.elsevier.com/locate/jnoncrysol

Investigation of atmospheric corrosion by photon energy dependent luminescence and Raman spectroscopy in aged and freshly fractured g-,c-As_2S_3 with photosensitive realgar inclusions

V. Mitsa [a], R. Holomb [a,*], A. Marton [a], M. Veres [b], S. Tóth [b], L. Himics [b], A. Lorinczi [c], M. Popescu [c]

[a] Institute of Solid State Physics and Chemistry, Uzhhorod National University, 88000 Uzhhorod, Ukraine
[b] Wigner Research Centre for Physics, Hungarian Academy of Sciences, 1121 Budapest, Hungary
[c] National Institute of Materials Physics, Magurele, Ilfov, Romania

ARTICLE INFO

Article history:
Received 18 July 2016
Received in revised form 21 September 2016
Accepted 22 September 2016
Available online xxxx

Keywords:
Atmospheric corrosion
As_2S_3 glass
Realgar
Pararealgar
Photoluminescence
Surface defects

ABSTRACT

We have studied the light emission properties of aged glassy (g-) and crystalline (c-) As_2S_3 and freshly fractured glassy As_2S_3 with photosensitive realgar inclusions in the 1.5–4.5 eV spectral range and applying different excitation photon energies. Additionally, Raman scattering measurements were performed on g-$As_{40}S_{60}$ to investigate structural changes caused by corrosion of the glass in air. Major features in the luminescence spectra were observed at 1.65, 1.87, 2.04, 2.26, 2.80 and 3.25 eV photon energies. The 1.65 eV band in photoluminescence spectra of g-As_2S_3 was identified to be related to the As side by comparison of the photoluminescence spectrum with literature data for As_4S_4 realgar crystal. A newly observed band at 1.87 eV was assigned to the As side in pararealgar occurring due to the light induced transformation from realgar to pararealgar phase. An oxidation process was found to take place during the aging and photo-aging accompanied with formation of As oxides, indicated by the emission bands at 2.04 and 2.26 eV. A rapid photo-oxidation process was observed in freshly fractured surfaces at room temperature which was connected with the light stimulated realgar-pararealgar transformation.

1. Introduction

From the middle of the '50s of the last century As_2S_3 glasses have attracted increasing attention in field of optical applications for near and mid-infrared region [1,2]. First investigations revealed that the arsenic sulfide glass has very low hygroscopicity, being a favorable characteristic to use it in optical elements [3]. However, the transparency has been reduced in infrared (IR) region for some samples due to internal impurities related to CO_2, OH, CS, H_2O groups [4–7]. During the use of glassy semiconductors for acusto-optical applications it was found that the presence of carbon, OH hydroxyl groups and molecular water is responsible for increasing sound attenuation, and these groups can appear in any glass composition [5]. However, additional purification of the initial elements before the preparation of the chalcogenide glasses (ChG) was found to decrease the internal impurity content and leaded to the commercialization of ChG for IR optical elements in many fields of practical applications [4–7]. But the level of purification by distillation was not satisfactory for application of ChG in form of fibers, where the limit of impurities content for $As_2S(Se)_3$ glass is predicted as follows (in ppm wt): <0.1 carbon, <0.5 hydrogen as CH group, <0.5 silicon, <0.1 metals [6–9].

There are many reasons for interest in the light guiding that can be used in numerous potential applications such as biological and chemical sensing, non-linear optics, pyrometers, and transmission of IR lasers [7, 9–11]. The efficiency and the stability of ChG in bulk, fiber and film forms are connected with optical aging due to the exposure to atmospheric conditions [7–15]. Unforeseen problems sometimes arise because of temperature changes, which may lead to the condensation of the moisture. The optical aging of fibers was established and associated with a dynamic grow of the absorption bands attributed to OH and H_2O groups [9]. Similar processes were observed in a bulk As_2S_3, for which the 2–4 μm wavelength region was the most affected one and a gradual degradation over the corrosion time was detected [14]. An ambient air exposure, in general, attacks the as prepared surface of the As_2S_3 films resulting in the formation of As_2O_3 crystals [12,13]. Beside internal impurities there are realgar nanophase inclusions in glassy matrix of g-As_2S_3 [15,16]. Illumination of g-As_2S_3 with realgar inclusions by laser beams of different photon energies causes polymorph realgar-pararealgar transition in the glassy matrix [15]. The effectiveness of this transformation depends mainly on the irradiation source (polychromatic or coherent monochromatic) [17] and on the photon energy used for the irradiation but the tendency was observed for all applied photon energies from 1.65 to 2.54 eV [18]. Both in case of exposure to ambient air and to light the realgar crystal shows a polymorph transition and formation of As_2O_3 units [19].

* Corresponding author.
E-mail addresses: v.mitsa@gmail.com (V. Mitsa), holomb@gmail.com (R. Holomb).

http://dx.doi.org/10.1016/j.jnoncrysol.2016.09.022
0022-3093/

In ambient conditions the ultraviolet light illumination induces oxidation of amorphous As_2S_3 film [20]. Generally, arsenic can be found in >320 minerals [21,22], including orpiment (As_2S_3) and realgar (r-As_4S_4), which were used as paint pigments formerly. Nowadays there is an issue connected with difficulties in finding the best illumination method for artworks belonging to the cultural heritage [21,22]. In nature, the arsenic bearing sulfides are oxidized and the increasing concentration of the dissolved arsenic can produce serious environmental problems [23]. It was found that general dissolution behavior and products for amorphous As_2S_3 and orpiment are comparable and differ only in terms of pH-dependency, reaction kinetics, and efficacy with generally lower activation [23–26]. In [24] it was concluded that hydroxide ions adsorb on the As_2S_3 surface, leading to the direct formation of arsenite ($HAsO_3^{2-}/AsO_3^{3-}$) and sulfide (S^{2-}) ions. Therefore, the problem of diagnostic of atmospheric corrosion product of chalcogenide glasses is multidisciplinary. The process is not completely clarified so far. The aim of this work is the investigation of excitation photon energy dependent photoluminescence and Raman scattering properties of aged g-,c-As_2S_3 and freshly fractured g-As_2S_3 contained photosensitive realgar inclusions.

2. Materials and methods

The glasses of As—S binary system were synthesized by the conventional melt quenching route in evacuated quartz ampoules from mixture of additionally purified by distillation in a vacuum (99.999%) As and S precursors. The synthesis were carried out at T = 1000 K for 10 h in a rotated ampoules. The melt quenching were performed from 1000 K and using a cooling rate of 1 K/s. The homogeneity of the prepared glasses were confirmed by polarization method. During the quenching of the melt the dissociation reaction of As_2S_3 at high temperature leads to the formation of additional nanophase inclusions of realgar in the glassy matrix, which is a main difference compared to quenching from low temperature [27].

Both aged and freshly fractured surfaces of As_2S_3 glasses were used for the investigation. The aging time for the As—S samples was ~ 10 years at T = 18–20 °C and humidity of about 60–70%. Crystalline As_2S_3 with visible α-As_4S_4 realgar inclusions and c-As_2S_3 without it were taken from Institute of semiconductor physics of National Academy of Sciences of Ukraine. The structure of these crystals were investigated elsewhere [28].

Photoluminescence emission spectra were recorded at room temperature, using different excitation wavelengths from a 450 W xenon arc lamp, selected by double monochromator system. Different bandpass filters were placed before the entrance slit of the detecting monochromator to separate the excitation beam and to avoid the appearance of its second order harmonics in the recorded spectra. The photoluminescence (PL) measurements were performed on a FL 3-22 type Horiba Jobin Yvon spectrofluorometer. A detailed measurement process of Raman spectra was described earlier [15,16].

3. Results and discussion

3.1. Excitation photon energy dependent Raman and photoluminescence of As_2S_3 glass

The Raman spectra of As_2S_3 glass excited with different photon energies is shown in Fig. 1 together with the spectra of polycrystalline As_2S_3. In contrast with narrow Raman bands of polycrystalline As_2S_3 located at 200, 290, 310, 355 and 383 cm^{-1} the Raman spectra of g-As_2S_3 demonstrate a broad band with the maximum at 340 cm^{-1}. The main band in the experimental spectra of As_2S_3 glass excited with photon energy of 1.17 eV (Fig. 1, curve 1) centered at 340 cm^{-1} is a characteristic band of symmetric As—S vibrations in AsS_3 pyramids. The shoulders at 310 and ~390 cm^{-1} is connected with the asymmetric As—S vibrations in AsS_3 pyramids and As—S—As vibrations of "water-like" molecule,

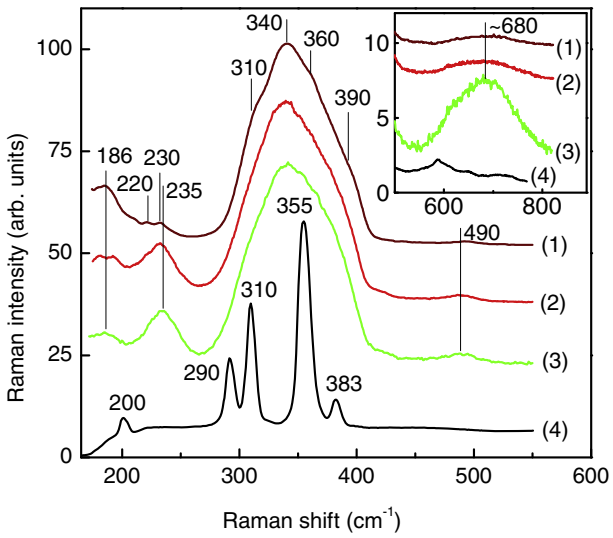

Fig. 1. The micro-Raman spectra of g-$As_{40}S_{60}$ excited by (1) $E_{ex.1}$ = 1.17 eV, (2) $E_{ex.2}$ = 1.96 eV and (3) $E_{ex.3}$ = 2.41 eV laser photon energies. The micro-Raman spectra (4) of polycrystalline As_2S_3 is shown at the bottom for reference.

respectively. In addition to these bands the small features at 186, 220, 230 and 360 cm^{-1}, connected with homopolar As—As bonds and realgar As_4S_4 inclusions, and small intensive band at 490 cm^{-1} associated with S—S bonds can be observed [17]. Drastic changes in the Raman spectra of As_2S_3 glass are observed when excitation photon energy increases (Fig. 1, curves 2 and 3). The decreasing of intensity of Raman band at 186 cm^{-1} and simultaneous increasing of ~235 cm^{-1} Raman band can indicate the realgar-pararealgar transformations [17,18]. Taking into account the strong absorption at these photon energies the changes in the Raman spectra can also be connected with the structure of glass surface. Using the excitation photon energy of 2.41 eV the broad band with maximum at ~680 cm^{-1} in the high frequency region of the Raman spectra of As_2S_3 glass is found to increase in intensity in comparison with the Raman spectra excited with lower photon energies (see inset in Fig. 1).

In addition to the Raman spectra, the excitation photon energy dependent PL spectra of As_2S_3 glass were investigated. The PL spectra of g-As_2S_3 excited with different photon energies is shown in Fig. 2. Results show that the main intensive band at ~2.80 eV in the PL spectra of aged As_2S_3 glass is observed when excitation photon energy of 3.10 eV is used (Fig. 2, curve 2). In addition to this band the bands at 1.65, 1.85, 2.04,

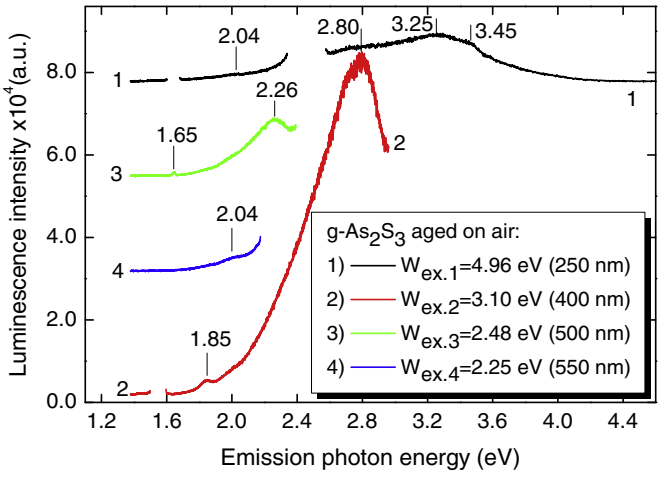

Fig. 2. The PL spectra of g-As_2S_3 aged on air recorded using different excitation photon energies (see inset).

2.26, 3.25 and 3.45 eV can be observed in the experimental PL spectra of As_2S_3 glass excited with different photon energies. (see Fig. 2). The microscopic structural origin of these PL features and it connection with aging and photo-induced processes will be discussed in next paragraph.

3.2. Luminescence from aged surfaces of g- and c-As_2S_3

The PL spectra of the fractured surface of g-As_2S_3, aged on air for long term and containing β-As_4S_4 realgar nanophase inclusions, excited with $W_{ex.2} = 3.1$ eV ($\lambda_{ex.2} = 400$ nm) is dominated by a relatively broad emission band having maximum around 2.80 eV (Fig. 2). The observed feature is typical for PL spectra of $As_2O_3 \times nH_2O$ solution [29]. In Raman spectra (Fig. 1) recorded by $E_{ex.3} = 2.41$ eV laser excitation, an energy that is very close to the band gap of the investigated material, a weak and broad scattering band centered near 680 cm^{-1} can be observed [15]. The broad feature is probably related to the superposition of two bands at 710 and 655 cm^{-1}, commonly observed for H_3AsO_3 and $As(OH)_3$ [30,31]. Such bands were detected in solutions saturated with As_4O_6 (pH = 0–4) and also in solutions where the ratio of [OH^-] and [As^{3+}] is equal to 3.5 [31]. In accordance with the Pourbaix's diagrams of As and S in water, at acidic conditions and in the presence of oxygen, the As_2S_3 compound reacts with water and the main reaction products are H_3AsO_3, H_3AsO_4, H_2S and H_2SO_4 [32].

A decrease of the excitation photon energy to $W_{ex.3} = 2.48$ eV ($\lambda_{ex.3} = 500$ nm) causes an increase of the emission intensity at lower energy region of the PL spectrum (Fig. 2, curve 3). As a result, a well distinguishable emission band appears at $E_2^* = 2.26$ eV accompanied by a weak shoulder around $E_1^* = 2.04$ eV on the low energy side of the mentioned band. These two bands can be identified as a signature of the As_2O_3 and As_2O_5 oxide phases, which usually appears in form of two separated bands in the PL of electrochemically etched porous eep-GaAs [33–35]. Since the As oxides have high optical band gap (~4–5 eV) the nature of the luminescence centers is still unknown. A possible explanation might be a mechanism similar to the observed PL bands in GeO_x, where they are related to defect sites [36].

The decrease of the excitation photon energy down to $W_{ex.4} = 2.25$ eV ($\lambda_{ex.4} = 550$ nm) results in a more pronounced shoulder around $E_1^* = 2.04$ eV in the PL spectrum of the aged sample (Fig. 2, curve 4). Comparing the PL spectra excited by 2.25 eV of glassy and crystalline As_2S_3 (Figs. 2 and 3, respectively) it is clearly seen that the typical emission band at $E_1^* = 2.06$ eV is much more pronounced for later structure. As was mentioned above, such PL band always appears in the PL spectra of oxidized porous GaAs and can be assigned to the presence of the arsenic oxide phase in the structure [33,34].

The use of higher excitation photon energies (4.96 eV (250 nm) for g-As_2S_3 and 4.59 eV (270 nm) for c-As_2S_3) results in a wide emission band ranging from 1.7 to 4.0 eV in both PL spectra with maxima around 2.80 and 3.25 eV for crystalline and glassy materials, respectively (Figs. 2 and 3). In contrast of g-As_2S_3 (Fig. 2), this band has a more complex structure in c-As_2S_3, which cannot be resolved at room temperature. Presumably, the experimentally obtained wide band is an envelope of many overlapped emission bands, including the $E_1^* = 2.06$ eV and $E_2^* = 2.26$ eV (Fig. 3) ones.

The maximum emission peak of g-As_2S_3 at $W_{ex.1} = 4.96$ eV (250 nm) excitation is located at 3.25 eV. Also, the few shoulders appear at 2.80 and 3.45 eV together with very weak feature at 2.04 eV (Fig. 2, curve 1). In this region As related bands were observed at 3.348 eV for the heavily As-doped ZnO film [37]. The As_2O_3 bands responsible for low temperature emission were observed in As-doped ZnO at 3.313, 3.232, 3.162, and 3.096 eV, but in the room temperature spectrum only a wide PL band can be seen near 3.3 eV [37]. The cathodoluminescence data obtained for bulk As_2O_3 show the emission line at 3.78 eV which was related with local As_2O_3 groups [38].

Thus in general can be stated that the PL spectra of aged c-As_2S_3 (Fig. 3) contain emission bands with almost the same positions as the PL spectra of aged g-As_2S_3 (Fig. 2), but the dominated relative intensities at different excitation energies are noticeably distinct. Previous investigation of oxidation of crystalline and amorphous phases of As_2S_3 shows that oxidation rate of c-As_2S_3 is slightly lower and the activation energy is higher, and the amorphous phase of As_2S_3 shows higher dependency on pH than the crystalline, and their reaction mechanisms for oxidation might be different [23–26]. Comparison of the PL spectra of g- and c-As_2S_3 supports some conclusions of authors of [23], saying that the general dissolution products of amorphous As_2S_3 and orpiment are comparable.

3.3. Intrinsic impurities or surface contamination effect during photo-aging

PL results for g-As_2S_3 measured at liquid nitrogen (curve 2) and room temperature (curve 1) are shown on Fig. 4. The observed maximum at E = 1.26 eV follows the well-known $E_g/2$ rule and reflects bulk intrinsic properties of the glassy material. The shoulder at 0.8 eV (see Fig. 4) which usually appears in the PL spectra of As—S glasses after UV light illumination is related to As atoms [39], while appearance of the shoulder at 1.72 eV may be connected with nanophase As_4S_4 realgar inclusion in the g-As_2S_3 matrix. A band with similar maximum was found in the PL spectrum of natural realgar crystal measured using 480 nm excitation [40]. A relatively weak PL band with maximum

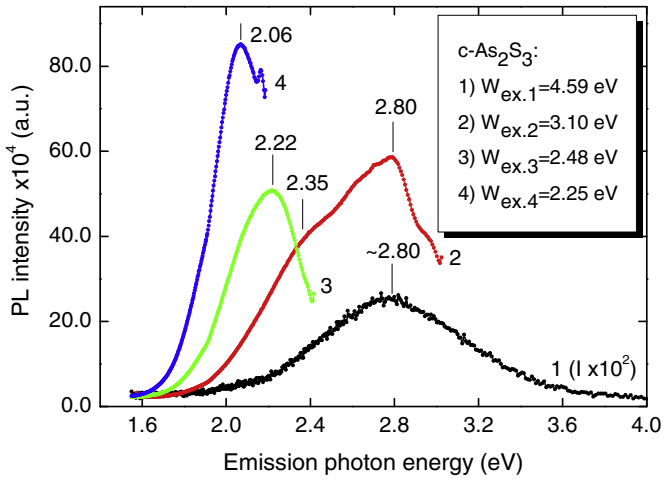

Fig. 3. The PL spectra of c-As_2S_3 with realgar inclusion aged on air, excited with different excitation photon energies (see inset).

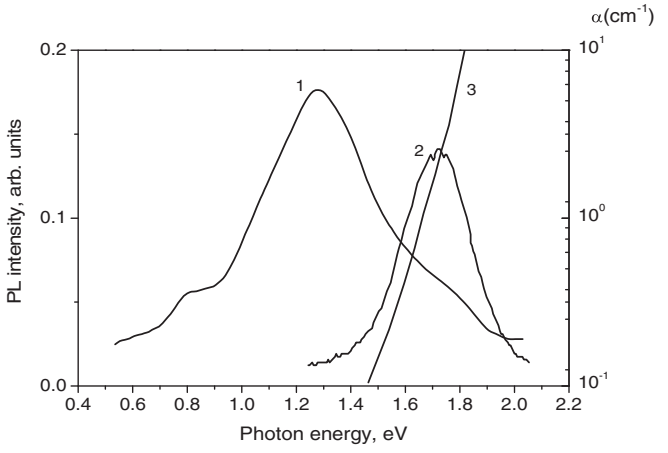

Fig. 4. PL spectra of g-As_2S_3 exited by wide band projector lamp and recorded at temperature of liquid nitrogen (curve 1) and excited by blue (403 nm) laser excitation and measured at room temperature (curve 2). Curve 3 represents the weak tail of absorption edge of g-As_2S_3 measured at room temperature

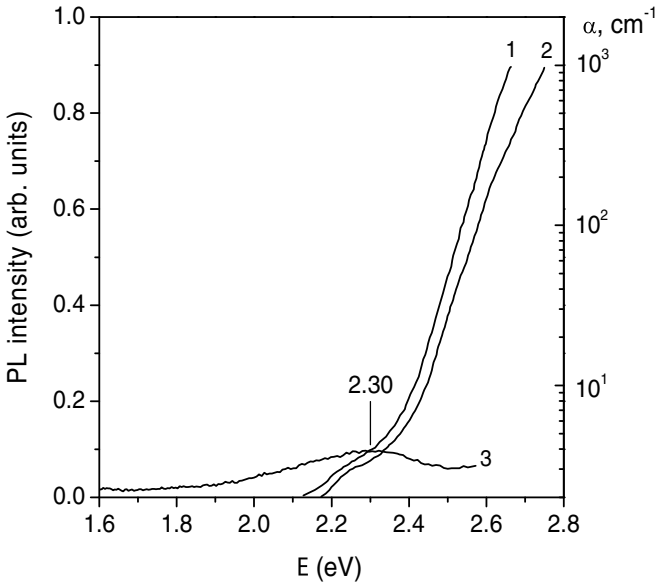

Fig. 5. The edge of the absorption for different polarizations of crystalline As_2S_3 (curves 1 and 2) recorded at room temperature [41]. The PL spectra of c-As_2S_3 recorded at room temperature using blue (403 nm) laser excitation (curve 3).

at 1.72 eV was observed in the spectrum of the freshly fractured g-As_2S_3 surfaces (see Fig. 4) measured with 403 nm laser excitation, the position of which is almost identical to the PL band in the emission spectrum of the realgar crystal [40]. Therefore, the observed PL band with maximum at 1.72 eV can be assigned to the As side in realgar. In contrast, the PL spectrum of g-As_2S_3 at liquid nitrogen temperature exited by wide band projector lamp shows mainly the bands connected with intrinsic properties of g-As_2S_3 (Fig. 4). All visible and near UV PL emission bands observed in the spectra measured at different excitation energies (Fig. 2) might be connected with surface contaminations.

The emission band at 2.30 eV, related to the As-oxide appears in the 403 nm laser excited PL spectrum of aged c-As_2S_3 without visible realgar inclusions. This emission band is significantly red shifted in comparison with edge of absorption of the c-As_2S_3 (Fig. 5). The oxide formation can serve as the physical reason for the surface degradation of g- and c-As_2S_3 during the aging process. Furthermore, the dissolution of the oxide and the formation of PL band assigned to $As_2O_3 \times nH_2O$ solution (the corresponding band is at 2.80 eV) may also occur in c-As_2S_3 (see Fig. 3, curves 1 and 2) because of the temperature variation during the aging process, which can cause the condensation of the moisture.

Formation of oxide phases during the aging of the fractured surface of the g-As_2S_3 with β-As_4S_4 realgar nanophase inclusions can be enhanced by the photo-aging [15,19]. The illumination of the g-As_2S_3 sample with UV laser resulted in the appearance of an emission band with maximum at $E_1 = 1.72$ eV (Fig. 4, curve 2). This PL band was assigned to As sides in realgar and has a blue shift with the illumination time to $E_2 = 1.87$ eV in the PL spectra of freshly fractured As_2S_3 glass measured using excitation photon energies of 2.25 and 2.48 eV (Fig. 6, curves 2). Common considerations of the excitation photon energy dependent Raman spectra (Fig. 1) and PL measurements of the freshly fractured g-As_2S_3 (Fig. 6) lead to the conclusions that the blue shift from E_1 to E_2 are presumably connected with the realgar-pararealgar transformation [15].

Therefore, using excitation energy $W_{ex.4} = 2.25$ eV at which the polymorphic transformation of realgar to pararealgar intensively occurs [15], the emission maximum shifts from E_1 to $E_2 = 1.87$ eV (this peak we assigned to *p*-As_4S_4) and, in addition, a new feature appears as a shoulder at $E_1^* = 2.04$ eV (As_2O_3) (Fig. 6, curve 2). The photo-degradation of the surface during the increase of the excitation energy to $W_{ex.2} = 3.10$ eV, accompanied with the formation of the emission band near 2.80 eV is less intensive as during the long term aging on air (Fig. 6, curves 1 and 2). Similar PL bands at 2.80 and 1.72 eV were found in PL spectra of crystalline auripigment As_2S_3 and *r*-As_4S_4, respectively. The shoulder at 3.75 eV observed in the PL spectra of g-As_2S_3 measured using excitation photon energy of 4.96 eV (Fig. 6) can be related with line at 3.78 eV detected in cathodoluminescence and indicating the formation of local As_2O_3 groups in bulk As_2O_3 [38].

4. Conclusions

The PL spectrum of the g-As_2S_3 investigated at liquid nitrogen temperature has a classical character. Emission band with maximum at $E = 1.26$ eV follows the well-known half optical band gap $E_g/2$ rule, being typical for intrinsic properties of glassy materials. The shoulders at 0.8 and 1.7 eV in the spectrum were assigned to the presence of As side nanophase inclusion in g-As_2S_3 matrix.

A low intensity PL band with maximum at 1.72 eV was observed in room temperature PL spectrum of g-As_2S_3 exited by 4.03 eV. The maximum position of this PL band is located on the so called weak edge absorption tail of the g-As_2S_3 spectrum. The prolonged illumination of the sample by UV light (4.03 eV) caused a blue shift of the emission band from 1.72 to 1.87 eV. This significant change in the PL peak position is presumably connected with the nanophase realgar to pararealgar transformation process stimulated by light illumination and observed earlier in g-As_2S_3.

Different surface contaminations were found in aged on air glassy and crystalline As_2S_3 during the analysis of the PL spectra excited by different photon energies. PL bands, belonging to red, yellow-green spectral regions are present in the PL spectra of both crystalline and glassy materials and are typical for arsenic oxides (As_2O_3 and As_2O_5).

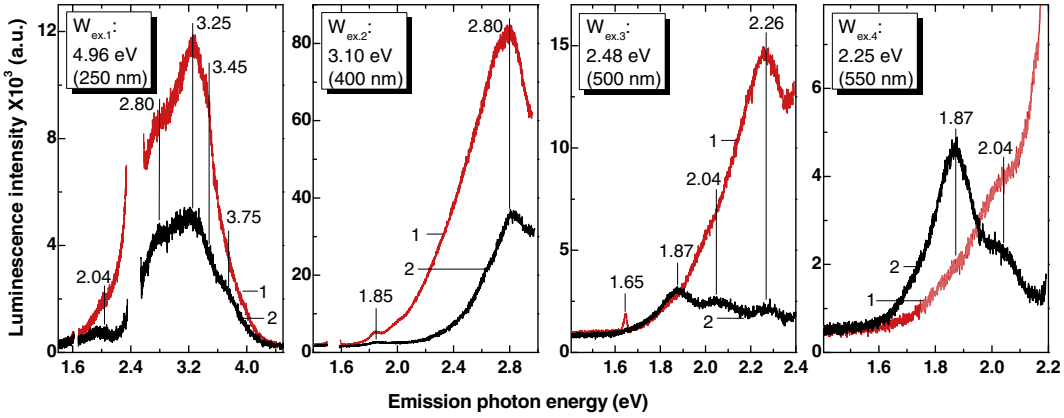

Fig. 6. Comparison of excitation photon energy dependent PL spectra of the aged (1) and freshly fractured (2) g-As_2S_3. The excitation photon energies are shown in the inset.

We have demonstrated that the position of PL bands related to the oxide phases in the emission spectra of crystalline c-As_2S_3 is the same as that of peculiarities on the low energy side of the edge absorption for c-As_2S_3. Therefore, the oxide growth may serve as the first step of surface degradation of g- and c-As_2S_3 during the aging on air.

It was established that during the aging process the temperature variations lead to the condensation of the moisture and active dissolution of the oxide phases at the surfaces of g- and c-As_2S_3. The dominant emission band around 2.80 eV, appearing in the PL spectra of g-As_2S_3 excited by different photon energies may be assigned to the $As_2O_3 \times nH_2O$ solution. Characteristic features of $As(OH)_3$ were observed in Raman spectrum of g-As_2S_3 excited with near band gap photon energies.

The analysis of the PL spectra of freshly fractured g-As_2S_3 surfaces with realgar nanophase inclusion demonstrated that the photo-aging caused by the realgar to pararealgar transformation is accompanied by simultaneous formation oxide phases. The appearance of a PL band typical for $As_2O_3 \times nH_2O$ was observed during UV excitation of the freshly fractured g-As_2S_3 surfaces. Intensities of PL bands from freshly fractured surfaces are at least few times lower compared to those measured on aged on air surfaces.

Acknowledgments

R.H. gratefully acknowledge support from the Hungarian Academy of Sciences within the Domus Hungarica Scientiarum et Artium Programme (2937/17/2016/HTMT). A.M. acknowledges a scholarship No-51600222 from the International Visegrad Fund within EaP program for this project at the Department of Applied and Non-linear Optics, Wigner Research Centre for Physics.

References

[1] R. Frerichs, New optical glasses with good transparency in the infrared, J. Opt. Soc. Am. 43 (1953) 1153–1157.
[2] V.A. Fraser, J. Jerger, Arsenic trisulfide: a new infrared transmitting glass, J. Opt. Soc. Am. 43 (1953) 322A–325A.
[3] F.W. Glaze, D.H. Blackburn, J.S. Osmalov, D. Hubbard, M.H. Black, Properties of arsenic sulfide glass, J. Res. Natl. Bur. Stand. 59 (1957) 83–92.
[4] C.T. Moynihan, P.B. Macedo, M.S. Maklad, R.K. Mohr, R.E. Howard, Intrinsic and impurity infrared absorption in As_2Se_3 glass, Non-Cryst. Solids 17 (1975) 369–385.
[5] Y.-F. Niu, J.-P. Guin, A. Abdelouas, T. Rouxel, J. Troles, Durability of an As_2S_3 chalcogenide glass: optical properties and dissolution kinetics, J. Non-Cryst. Solids 357 (2011) 932–938.
[6] S. Danto, D. Thompson, P. Wachtel, J.D. Musgraves, K. Richardson, B. Giroire, A comparative study of purification routes for As_2Se_3 chalcogenide glass, Int. J. Appl. Glas. Sci. 4 (2013) 31–41.
[7] M. Popescu, A. Lőrinczi, F. Sava, M. Stegărescu, M. Iovu, M. Leonovici, T. Halm, W. Hoyer, Structure and properties of $As_{25}Te_{35}Si_{40}$ glass, J. Non-Cryst. Solids 326–327 (2003) 389–393.
[8] D.M. Kane, R.J. Chater, D.B. Gore, D.S. McPhail, Corrosion at the surface of chalcogenide glass microspheres, J. Opt. 14 (2012) 055401 (8pp).
[9] O. Mouawad, C. Strutynski, J. Picot-Clémente, F. Désévédavy, G. Gadret, J.-C. Jules, F. Smektala, Optical aging behaviour naturally induced on As_2S_3 microstructured optical fibres, Opt. Mater. Expr. 4 (2014) 2190–2203.
[10] V. Mitsa, R. Holomb, M. Veres, A. Marton, I. Rosola, I. Fekeshgazi, M. Koós, Non-linear optical properties and structure of wide band gap non-crystalline semiconductors, Phys. Stat. Sol. C. 8 (2011) 2696–2700.
[11] M. Popescu, A. Velea, A. Lőrinczi, M. Zamfirescu, F. Jipa, S. Micloş, A. Popescu, M. Ciobanu, D. Savastru, Two dimensional photonic structures based on As-S chalcogenide glass, Dig. J. Nanomater. Biostructures 5 (2010) 1101–1105.
[12] J.S. Berkes, S.W. Ing Jr., W.J. Hillegas, Photodecomposition of amorphous As_2Se_3 and As_2S_3, J. Appl. Phys. 42 (1971) 4908–4916.
[13] P.J. Allen, B.R. Johnson, B.J. Riley, Photo-oxidation of thermally evaporated As_2S_3 thin films, J. Optoelectron. Adv. Mater. 7 (2005) 1759–1764.
[14] Y.-F. Niu, J.-P. Guin, A. Abdelouas, T. Rouxel, J. Troles, Durability of an As_2S_3 chalcogenide glass: optical properties and dissolution kinetics, J. Non-Cryst. Solids 357 (2011) 932–938.
[15] R. Holomb, V. Mitsa, P. Johansson, N. Mateleshko, A. Matic, M. Veresh, Energy dependence of light-induced changes in g-$As_{45}S_{55}$ during recording the micro-Raman spectra, Chalcogenide Lett. 2 (2005) 63–69.
[16] O. Shpotyuk, S. Kozyukhin, Y. Shpotyuk, P. Demchenko, V. Mitsa, M. Veres, Coordination disordering in near-stoichiometric arsenic sulfide glass, J. Non-Cryst. Solids 402 (2014) 236–243.
[17] R. Holomb, V. Mitsa, O. Petrachenkov, M. Veres, A. Stronski, M. Vlček, Comparison of structural transformations in bulk and as-evaporated optical media under action of polychromatic or photon-energy dependent monochromatic illumination, Phys. Stat. Sol. C. 8 (2011) 2705–2708.
[18] R. Holomb, N. Mateleshko, V. Mitsa, P. Johansson, A. Matic, M. Veres, New evidence of light-induced structural changes detected in As–S glasses by photon energy dependent Raman spectroscopy, J. Non-Cryst. Solids 352 (2006) 1607–1611.
[19] M. Zoppi, G. Pratesi, The dual behavior of the β-As_4S_4 altered by light, Am. Mineral. 97 (2012) 890–896.
[20] P. Knotek, M. Vlcek, M. Kincl, L. Tichy, On the ultraviolet light induced oxidation of amorphous As_2S_3 film, Thin Solid Films 520 (2012) 5472–5478.
[21] W.V. Davies, Color and Painting in Ancient Egypt, The British Museum Press, London, 2001.
[22] A. Macchia, L. Campanell, D. Gazzoli, E. Gravagna, A. Maras, S. Nunziante, M. Rocchia, G. Roscioli, Realgar and light, Procedia Chem. 8 (2013) 185–193.
[23] M.F. Lengke, R.N. Tempel, Reaction rates of natural orpiment oxidation at 25–40 °C and pH 6.8–8.2 and comparison with amorphous As_2S_3 oxidation, Geochim. Cosmochim. Acta 66 (2002) 3281–3291.
[24] A.K. Darban, M. Aazami, A.M. Meléndez, M. Abdollahy, I. Gonzalez, Electrochemical study of orpiment (As_2S_3) dissolution in a NaOH solution, Hydrometallurgy 105 (2011) 296–303.
[25] M.F. Lengke, R.N. Tempel, Arsenic sulfide oxidation at acid pH values, Trans. Soc. Min. Metall. Explor. 312 (2002) 116–119.
[26] M.F. Lengke, R.N. Tempel, Natural realgar and amorphous AsS oxidation kinetics, Geochim. Cosmochim. Acta 67 (2003) 859–871.
[27] K. Tanaka, Chemical and medium-range orders in As_2S_3 glass, Phys. Rev. B 36 (1987) 9746–9752.
[28] M.P. Lisitsa, U. Nasyrov, I.V. Fekeshgazi, Temperature effect on non-linear light absorption in arsenic sufide, Ukr. J. Phys. 22 (1977) 674–676.
[29] D.N. Goryachev, O.M. Sreseli, Photoluminescence of porous porous gallium arsenide, Semiconductors 31 (1997) 1383–1386.
[30] R.L. Frost, S. Bahfenne, A review of the vibrational spectroscopic studies of arsenite, antimonite, and antimonate minerals, Appl. Spectrosc. Rev. Int. J. Princ. Methods Appl. 45 (2010) 101–129.
[31] S.A. Wood, C.D. Tait, D.R. Janecky, Raman spectroscopic study of arsenite and thioarsenite species in aqueous solution at 25 °C, Geochem. Trans. 3 (2002) 31–39.
[32] M. Pourbaix, L. Pourbaix, Potential-pH equilibrium diagrams for the systems S–H_2O from 25 °C to 150 °C. Influence of access of oxygen in sulfide solutions, Geochim. Cosmochim. Acta 56 (1992) 3157–3178.
[33] C.M. Finnie, P.W. Bohn, Near-field photoluminescence of microcrystalline arsenic oxides produced in anodically processed gallium arsenide, Appl. Phys. Lett. 74 (1999) 1096–1098.
[34] M. Rojas-López, J.M. Gracia-Jiménez, M.A. Vidal, H. Navarro-Contreras, R. Silva-González, E. Gómez, Raman study of luminescent spark processed porous GaAs, J. Vac. Sci. Technol. B 19 (2001) 622–627.
[35] Z. Harrabi, L. Beji, N. Chehata, A. Ltaief, H. Mejri, A. Bouazizi, Effects of growth conditions on structural and optical properties of porous GaAs layers, J. Nanotechn. Adv. Mat. 2 (2014) 57–64.
[36] V. Mitsa, M. Ivanda, O. Gamulin, R. Holomb, O. Kondrat, N. Popovych, G. Lovas, S. Petreckiy, N. Tsud, V. Matolín, K.C. Prince, Luminescence, Raman and Synchrotron XPS Study of Amorphous Ge_2S_3 Based FilmsProceedings of the 35thInternational convention on information and communication technology, electronics and microelectronics 2013, pp. 34–39 MIPRO 2013/MEET.
[37] T.S. Jeong, J.H. Kim, S.J. Bae, M.S. Han, C.J. Youn, Re-crystallization and characteristic As properties of As-implanted ZnO activated by ozone at various annealing temperatures, Int. J. Kor. Phys. Soc. 49 (2006) 2316–2320.
[38] S.W. McKnight, E.D. Palik, T.N. Bhar, Cathodoluminescence studies of anodic oxides on GaAs, J. Vac. Sci. Technol. 17 (1997) 967–970.
[39] T. Tada, T. Ninomiya, Photoluminescence from optically induced metastable states in a-As_2S_3, J. Non-Cryst. Solids 114 (1989) 88–90.
[40] S.G. Bishop, B.V. Shanabrook, U. Strom, P.C. Taylor, Comparison of optically induced localized states in chalcogenide glasses and their crystalline counterparts, J. Phys. 42 (1981) 383–386.
[41] N.F. Mott, E.A. Davis, Electronic Processes in Non-Crystalline Materials, Clarendon-Press, Oxford, 1971.